Patient-specific 3D-printed Splint for Mallet Finger Injury

Ali Zolfagharian[1]*, Timothy M. Gregory[1], Mahdi Bodaghi[2], Saleh Gharaie[1], Pearse Fay[3]

[1]School of Engineering, Deakin University, Geelong 3216, Australia

[2]Department of Engineering, School of Science and Technology, Nottingham Trent University, Nottingham NG11 8NS, UK

[3]School of Health and Social Development, Deakin University, Geelong 3220, Australia

Abstract: Despite the frequency of mallet finger injuries, treatment options can often be costly, time-consuming, and ill-fitted. Three-dimensional (3D) printing allows for the production of highly customized and inexpensive splints, which suggests potential efficacy in the prescription of casts for musculoskeletal injuries. This study explores how the use of engineering concepts such as 3D printing and topology optimization (TO) can improve outcomes for patients. 3D printing enables the direct fabrication of the patient-specific complex shapes while utilizing finite element analysis and TO in the design of the splint allowed for the most efficient distribution of material to achieve mechanical requirements while reducing the amount of material used. The reduction in used material leads to significant improvements in weight reduction and heat dissipation, which would improve breathability and less sweating for the patient, greatly increasing comfort for the duration of their recovery.

Keywords: Patient-specific, Three-dimensional printing, Splint, Topology optimization

*Corresponding Author: Ali Zolfagharian, School of Engineering, Deakin University, Geelong 3216, Australia; a.zolfagharian@deakin.edu.au

1 Introduction

Mallet finger is one the most common upper limb athletic injury that may occur due to bony avulsion or tendentious lesion[1]. This injury could significantly affect individuals overall function, impairing their work-related skills and social capability to perform daily living activities[2]. The current treatment involves immobilizing the affected joint using a splint made of thermoplastic or plaster in a neutral position. The splint could be prefabricated; however, in most cases, a trained health professional cast a splint for the patient. Intrinsically, the outcome will be highly dependent on the skills and knowledge of the medical practitioner. Even with highly trained health professionals completing this, there are many factors that impact on the wearing of splints resulting in non-adherence and decreased outcomes[3]. In addition, it is a lengthy and labor-intensive process requiring the fabrication of multiple casts leading to excessive use of materials and efforts. Yet, additive manufacturing (AM) technology recently allows for the fabrication of individualized prosthetics based on patient anthropometrics[4].

Additively manufactured orthosis orthopedics for injuries treatments or rehabilitation are not currently in widespread use, though, it could potentially offer a way to reduce the cost of production and enable easy customization to an individual in biomedical treatments that addresses many of the current barrier to adherence[5,6].

Effective use of AM may lead to a reduction in size and weight of the splint making it more comfortable for the user. This paper presents an investigation into the use of a fused deposition modeling (FDM) printer to trial printing methods to produce a person and injury-specific mallet finger splint at a low-cost and optimized weight and comfortability.

1.1 Mallet finger injury

Mallet finger is the extremely common finger injury where the fingers extensor ability is disrupted at its terminal portion, causing an inability to extend at the distal interphalangeal joint[7]. This disruption is either due to rupture of the fingers extensor tendon or an avulsion fracture (fracture to the bone in a location where a tendon or ligament attaches)[8] of the distal phalange. Swelling and tenderness can occur together with reduced ability to extend the distal phalanx, resulting in extension lag of anywhere from a couple of degrees up to several dozen. The cause can be either direct blow to the distal phalanx, sharp, or blunt injury to the distal interphalangeal joint[9]. This injury is commonly seen in ball sports such as Basketball, Volleyball, and Cricket. Injuries to the lower arm, including hand and wrist, are extremely common, accounting for 20% of all emergency presentations[10].

The economic burden for these injuries is extensive with the direct, indirect, and intangible

costs associated and increases with the severity or complexity of the injury[10]. Although, in most cases, the patient will make a full recovery, often, a long period of recovery is required, and some will not recover full function and may potentially have a lasting disability (**Figure 1**). Mallet finger is often left untreated by patients unless severe restriction in extensor ability is present, or there is lingering pain[11]. This injury, in the case, that there are functional shortfalls, can impede the whole hand in everyday fine motor skill tasks. Furthermore, this deformity can develop additional medical conditions in the finger and hand as overcompensation can create hyperextension of proximal interphalangeal joint, a swan neck deformity[7].

The use of a movement restriction device called a splint is the common form of treatment for this injury. The splint is designed to hold the affected area of the finger in neutral or a small degree of hyperextension while the tendon or avulsion fracture can heal.

1.2 Current mallet finger treatments

The conservative and post-surgical management of mallet finger injuries require the use of splints to aid in recovery. Preventing any movement in the distal interphalangeal joint is crucial as flexion of the joint will separate the torn ends of the tendon or avulsion fracture, halting the recovery process. In this case, the finger would need to be returned to full extension, and the healing process would start again from the beginning. There are several types of splints that can be used for this condition; the three commonly used splints are the stack (prefabricated), dorsal aluminum, and personalized thermoplastic splints (**Figure 2**).

Beyond the use of the dorsal aluminum splint, there are specifically designed mallet finger splints
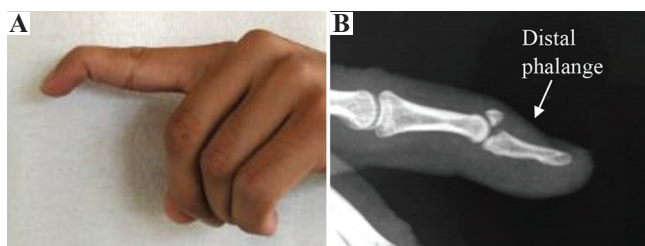
Figure 1. (A) Mallet finger fracture (Image courtesy from Sachin J Shah, MD, online), (B) anatomy of finger[12].

Figure 2. (A) Stack, (B) dorsal aluminum, and (C) personalized thermoplastic splints[13].

used in the treatment of this condition. Either cast molded products known as "off the shelf," which are manufactured in three ready-made sizes or personalized molded thermoplastic products that a health professional makes for the patient at the clinic. The stack splint is generally made from polypropylene and is largely enclosed with limited holes in the top section for airflow. The stack splint is applied to the patient's finger and then attached to the skin on the proximal phalange with skin tape or strapping tape to help prevent movement. However, the "off the shelf" splints embody a one size fits all approach which cannot accommodate all patients.

The dorsal aluminum splint is a commonly prescribed method for treating mallet finger. This method utilizes a splint on the dorsal section of the finger and then taped onto the finger at the distal phalange and the intermediate phalange. This method provides greater airflow than the stack splint as the ventral section of the finger and the fingertip is left open to the air. This theoretically provides an advantage over stack splint in that decreased pressure is exerted to the distal interphalangeal joint, allowing better blood supply[7].

Personalized thermoplastic splints are applied by trained health professionals, which involves taking the measurements of a patient's finger and then cutting a piece of thermoplastic to a specific splint design. The thermoplastic is heated, and the finger is wrapped in the thermoplastic with the tabs joining the piece over the top of the finger. Using scissors, a health professional can trim the ends further to better fit the patient. The thermoplastic conforms to the skin and sets when it cools, maintaining the finger in the position that it has been molded to. There are several complexities with this manufacturing process, including that the manufacturing process is manual and highly skill dependent. The splint received from a graduate health professional may be completely different in quality to the veteran therapist who has been creating these splints by hand for years. The splint, if poorly fitted, can result in shear stress, directional misalignment, and pressure over bony prominences[9]. A comparison study of these three

splints in the treatment of mallet finger has been reported by O'Brien[13]. All three types of splints are required to be worn for 6 – 8 weeks. Treatment failure or complications include skin irritation, poor splint fit, splint breakage, pain, or discomfort wearing the splint or patient dissatisfaction with splint appearance or cumbersome nature. When worn for the entirety of this period, there was no extensor lag difference found between the three splint types, but custom-made thermoplastic splints were significantly less likely to result in treatment failure[13].

This suggests that customized splints, fitted to the exact dimensions of a patient's finger, have the ability to provide successful treatment in more cases than the other two splint types. This finding propelled the current study to use AM technology to rapidly produce the personalized fitted shape splint customized to the patient. This technology could provide a standardized and efficient approach to manufacturing mallet splints that may reduce cost, improve adherence, and have less impact on patient's hand function while wearing the splint.

1.3 AM

AM is a promising and developing manufacturing method. Historically, AM technology was utilized for prototype creation; increasingly, however, it is being seen and has become a production technique in its own right[14,15]. The AM groups a large number of technologies and techniques that can utilize different materials with vastly differing properties to create parts for a range of applications[16].

The three-dimensional (3D) printing has become a large part of the new frontier of medical technology and treatment. Medical treatments that use 3D printing techniques include: Facial reconstruction, orthodontics, exoskeletons, prosthesis, tumor detection, chirurgical optimization and biocompatible organ, and tissue printing[17,18]. In the medical field, using traditional manufacturing methods take a lot of production time and are not easily customizable to patients; hence, its use is becoming more limited. FDM, also known as fused filament fabrication, is one of the most common AM technologies using numerous varieties of thermoplastic materials[19,20].

During the early years of the introduction of the FDM technique, it was used to print prototypes, souvenirs, and other useful domestic appliances[21,22]. However, FDM technology is rapidly maturing and is reportedly showing unlimited potential in various applications, including in the medical, automotive, and aeronautical fields[23-25]. FDM can benefit the mallet finger treatment through making complex shapes that could not be made by traditional manufacturing methods as well as its ability to utilize alternative materials with improved performance characteristics[7,26].

The first step of FDM printing is to develop a computer-aided drawing (CAD) of the component. That CAD file is then exported as a stereolithography (STL) file. This STL file is then "sliced" by the 3D printer's software and read by the printer to print the component in a series of layers[27]. FDM prints thin layers of plastic layer by layer to create the part. Plastic is fed into the extrusion head and then heated so that it enters a semi-liquid state; the plastic is then pushed out of a small nozzle to produce a fine thread of plastic that it layers onto the previous layer or onto the base support piece. Because of this layer on the layer structure of the material, the mechanical properties and surface finish of an FDM printed part are dependent on the orientation of which it is printed. This means even the same part can have different mechanical properties if printed in different orientations[28].

Despite previous studies into AM for use in lower limb prosthetics and orthotics, the use of 3D printing technologies for the use on the upper extremities of the arm, including wrist, hand, and fingers, has yet to be investigated broadly[11]. Up to the present time, there has been limited research in the area of upper extremity splinting with engineering design and analysis motivation[5,29].

The interest in 3D printing in this area is due to multiple reasons. One is the scalability with respect to the range of sizes. It is completely customizable to the patient's injury. In addition, multiple splints can be printed for the patient over the course of their recovery as swelling reduces to ensure the splint is optimally fitted at all times throughout their recovery[30]. This practice potentially provides the best outcome for the patient. Further, 3D printed splints can also be made to accommodate extremes of size or deformities that off the shelf splints cannot. Utilizing this technology means that a patient can receive the same quality of care regardless of the health professionals level of skill and experience in splint manufacturing immediately after an injury the patient gets their finger scanned and a medical professional selects the template for their finger injury that is then automatically updated with the exact dimensions of their finger. A personalized finger splint is then printed off, tailored to them exactly, to allow for the chance at the most optimal recovery followed by ongoing rehabilitation with a health professional.

The personalized FDM 3D-printed thermoplastic finger splint in this study could potentially address all those common causes of treatment failure, such as skin irritation, poor splint fit and discomfort wearing the splint, which would lead to less treatment failure and therefore more successful recovery cases.

2 Methodology

The goal of this study is to utilize the FDM method to develop a patient-specific 3D-printed finger splint that could potentially have the properties required to match and exceed those of the current hand-molded thermoplastic splints. The original splint will be compared with the topology-optimized splints in terms of structural and thermal performance. With these processes, splints can be produced with much better mechanical properties requiring less material for more breathability and comfort while having the same strength. The detailed steps of achieving this aim are outlined in the following.

### 2.1 Measurements of finger and personalized CAD splint

The patient-specific splint was designed by measuring seven parameters of a patient's index finger, as shown in **Figure 3**. To measure the maximum force that could be applied by the index finger, the intermediate and proximal joints of the finger were locked in position using medical tape to the bottom of the finger. This left the distal interphalangeal joint of the finger, the joint

affected by mallet finger, the only joint with a degree of freedom.

Using Autodesk Inventor Software and the measurements, the patient-specific splint is designed. As shown in **Figure 4**, a constraint was designed at the rear of the splint to prevent leeway in the splint when being worn. When the user clenches their fist, without this material removed, the skin of their middle phalanx finger can push into the back of the splint dislodging its correct position. The stack splint is designed with an open ventilation section above the fingernail to allow some airflow to reduce sweat when being worn and to allow limited access
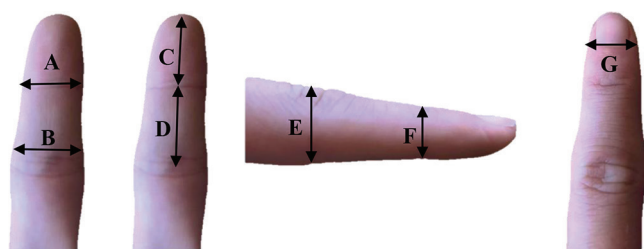
Figure 3. The seven measurements required to create a personalized finger splint computer-aided drawing model.
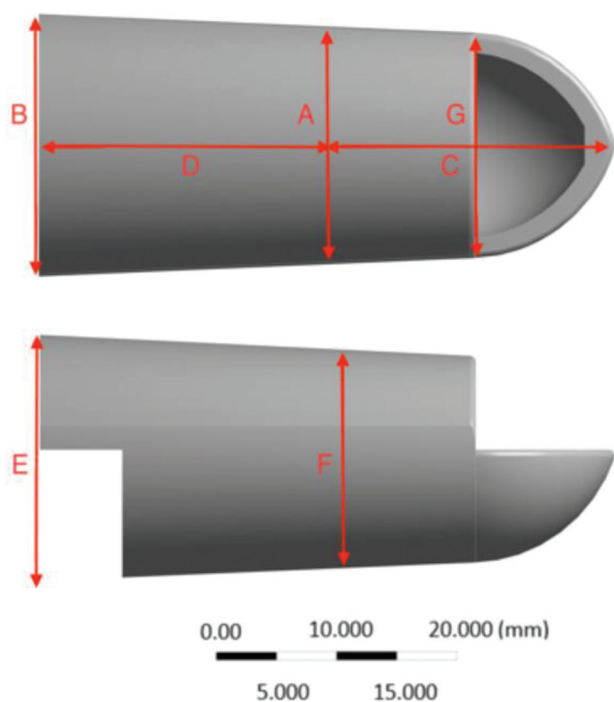
Figure 4. Geometry of a sample 100% mass design according to a patient's finger.

for washing. The top section of the splint extends to the proximal interphalangeal joint. This allows the user some flexion of the finger without hindering recovery. A benefit of using topology optimization (TO) is that areas of the finger and finger pad remain exposed, so a person can still feel and get sensation through the finger when performing everyday tasks such as writing with a pen or using their toothbrush. This is opposed to a molded splint that is fully enclosed, which makes the finger become less functional for the recovery period. The maximum pressure load calculated from the distal interphalangeal joint, simulating the maximum force a person could generate in their index finger solely from the flexion of the distal interphalangeal joint, was applied to the rim of the finger splint. This was chosen because the finger "pad" section of the splint is a large space that will be optimized in all topology-optimized splints. Because of this, the area and geometry in that section changed for each splint. By applying the pressure load to the rim of the splint, it was a consistent way to compare all splints.

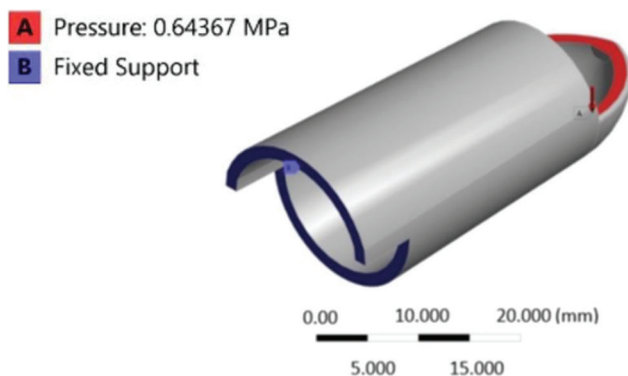## 2.2 3D Printing patient-specific finger splint

A number of materials could potentially be used in FDM having the properties required to match and exceed those of the current hand-molded thermoplastic splints. These materials include poly-lactic-acid (PLA), acrylonitrile-butadiene-styrene, polyamide, thermoplastic polyurethane, polycarbonates, polystyrene, and poly-ether-ether-ketone. Environmental considerations were considered as the use of this product is highly personal; it cannot be passed onto the next patient, so it must be disposed of after treatment. The non-recyclability of casts and splints causes large amounts of waste. In fact, in the US, according to the National Ambulatory Medical Care Survey and American Academy of Orthopaedics, 2.4% of the population experiences some fracture[31], producing an average of 670,000 kg of waste per year[17,32]. However, PLA being derived from natural sources, corn, beet, and cassava among others, is biodegradable. Because of this, PLA splints can be composted after their 6 – 8 weeks use, rather than

contribute to landfills. The PLA is used in this study as it has been found to be feasible for the production of scaffolds with different architectures and controlled porosities which are tailored for use as temporary fixtures in biomedical applications[33,34]. In addition, polyvinyl alcohol used as support materials, which is a water-soluble, biodegradable polymer under both aerobic and anaerobic conditions[35].

2.3 TO

TO is utilized here to create a series of splints optimized for the loading conditions. The original splint will be compared with the topology-optimized splints in mechanical performance and in thermal qualities that will affect the users' comfort experience. With these processes, splints can be produced with much better mechanical properties requiring less material, for more breathability and comfort, while having equal strength. In this study, a splint is developed based on TO in which the algorithm starts from a solid model of the material. Distributed loading and boundary conditions are defined based on the specifications of the splint finger, as shown in **Figure 5**. The main objective here is to remove the maximum material while preserving the volume fraction and maximum stiffness of the 3D-printed splint[36,37].

The theory of the optimality criteria (OC) is used in ANSYS Workbench. The OC method uses an estimation of the optimality conditions to update the design variables of each point[38]. The designs are updated independently using this method, the material is added in the areas in which the estimation of the strain energy is too high[39].

2.4 Finite element analysis (FEA) and mesh convergence

TO with the minimum compliance criteria was coupled with a structural analysis module in ANSYS 2019 R2 to evaluate varying splint designs. Since, the mechanical properties of the 3D printed parts are affected by the 3D printing parameters, for example, layer thickness and raster width, Young's modulus and Poisson's ratio of PLA were obtained according to Type I ASTM D638 test standard. PLA with a density of m^3, Young's modulus of 2850 MPa, and Poisson's ratio of 0.25 were defined for the material properties of the splint. The maximum pressure exerted was estimated to be 64×10^4 Pa applied at the rim of the splint, and the base was assumed to fix (**Figure 5**).

The domains of 100%, 79.49%, 71.13%, and 62.51% mass were discretized by unistructural tetrahedral elements with 394,439, 140,904, 104,634, and 104,026 elements, respectively, as shown in **Figure 6**, where higher mesh density was selected for the region of interest and local mesh refinement was conducted to achieve high mesh quality. Note that mesh independence studies were

Figure 5. Schematic view of boundary conditions on a sample splint design.
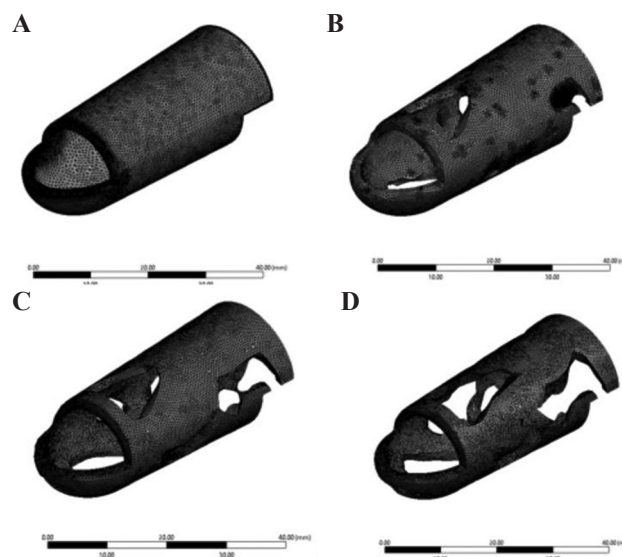
Figure 6. Domains discretization with tetrahedral elements for (A) 100%, (B) 79.49%, (C) 71.13%, and (D) 62.51% mass.

conducted with varying element sizes and model that had <5% variation in maximum stress was selected.

2.5 Thermal heat analysis

Using the four splints created, thermal analysis of the prototypes was undertaken. The Static Structural module in ANSYS used to test for deflection and stress values were linked with steady-state thermal module to link the data. The internal face of each of the splints was selected and set at 31.7°C, the temperature of the skin at room temperature[40]. The convection coefficient of air at 22°C in free convection was selected as 10 W/(m².K). The total heat generation of the human body for this project is selected 110 W[41]. A heat flux was also created for the internal face assuming that the average body surface area of human adult is 2 m². **Table 1** details the properties calculated above.

To clarify, for the topology-optimized splints, meshing was done for TO using a low element number, default mesh. Once the topology-optimized shape was obtained, it was then inserted into back into static structural, and a new refined mesh with a high number of elements was used to ensure that data values obtained regarding deflection, stress, and heat are as accurate as possible.

3 Results and discussion

The low-cost 3D printer used in this study was the Ultimaker2 Extended+ (Ultimaker B.V., Geldermalsen, The Netherlands). The splints were printed at 100% infill, nozzle speed of 20mm/s, heat bed of 50°C, and layer thickness of 0.2 mm. The dog-bone type PLA samples were 3D-printed according to Type I ASTM D638 with a width of 13 mm, the thickness of 5 mm, and a gauge length of 50 mm. To determine basic mechanical properties, tensile tests, as shown in **Figure 7**, were conducted on 3D-printed dog-bone specimens. The tests were performed in an Instron 300LX (Instron, High Wycombe, UK) with a crosshead speed of 5 mm/min. Tensile

Table 1. Heat simulation analysis settings

Internal splint surface temperature (°C)	31.7
Convection coefficient of air $\left(\dfrac{W}{m^2 \cdot K}\right)$	10
Total heat generation of human body (W)	110
Average body surface area of human adult (m²)	2
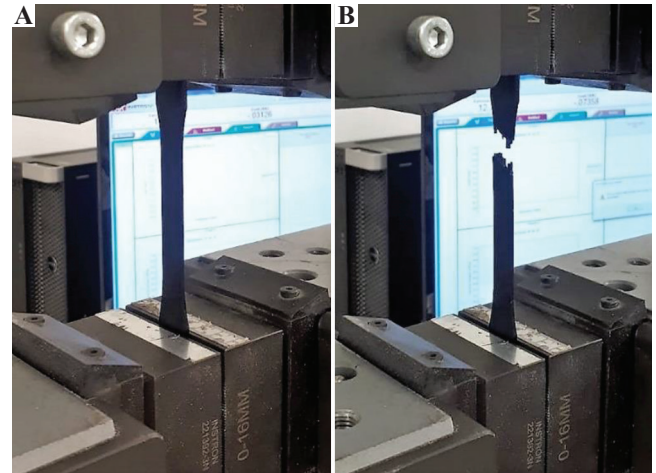
Figure 7. A three-dimensional-printed dog-bone poly-lactic-acid sample (A) before, and (B) after tensile test.

strength and modulus of the 3D-printed samples were determined 52.2 MPa and 2.86 GPa, respectively. In FDM topology optimized and original design, finger splints were fabricated, original (100% mass), 62.51% mass, 71.13% mass, and 79.49% mass, by the same 3D printer and processing parameters used for the dog-bone specimens (**Figure 8**).

To test the maximum deflection of the splints under realistic conditions, the rear of the splint was the fixed end with the load to be applied at the front of the splint near the tip of the finger. This was used to simulate how the splint would deform under the force applied solely by the final joint of the finger (distal interphalangeal joint). As the splint does not extend onto the second joint of the finger, only the force that could be produced by the final joint was considered. In FEA, the fixed support geometry was consistent across all simulations and excluded from TO. To complete the mesh convergence study, the measured force value was applied to the rim of the finger pad area.

Figure 8. From left to right 62.51%, 71.13%, 79.49%, and 100% mass splints.

The maximum deflection and maximum stress values were recorded for each mesh. Then, the mesh was refined, increasing the number of cells, and then the maximum deflection and maximum stress values were recorded again. Once both the deflection and maximum stress values were within 2% of previous deflection and stress values from the previous mesh, the mesh was called converged. This means the results obtained from any simulation can be assumed accurate enough that they are no longer significantly impacted by the mesh once mesh convergence was achieved off the original splint. Deflection and stress values were calculated through ANSYS simulation to establish the printable material with the best mechanical properties.

The stress and deflection simulation results of the splints are obtained and shown in **Figures 9 and 10**. All splints had stress concentrations at the corner between the finger pad rim and the rim of the enclosed top section. This was the location of the highest stress values for each splint. The highest values of deflection were obtained at the tip of the finger pad rim section. As would be expected when removing material from a loaded structure, its deflection increases as more material is removed. What is noteworthy though, according to **Figure 11A and 11B**, the 79.49% splint had a reduced mass of 20.51% but only deflected 0.24 mm, which was only 24% more than the original, 100% mass, splint. However, there appears to be an optimum percentage of mass reduction as the 71.13% splint

deflected 0.31 mm, which is almost 50% more than the 100% mass splint. This result shows that there is appoint of diminishing returns in removing material from the structure. This indicates the effectiveness of the TO in splint finger design.

In line with the increase in deflection as the splints had a reduction in material, the maximum stress values decreased. There was however an outlier in the 71.13% splint, which recorded 31.16 MPa that experienced the least stress among all. This result would appear as the objective of the TO in this study was set for the least deflection only.

The heat distribution results of the splints are also simulated and shown in **Figures 11C and 12**. With each iteration of the topology-optimized finger splint with less material, the average heat dissipation in the splint increased slightly as expected. The heat flux upturn in between splints was roughly proportional to the decrease in percentage mass to the previous splint, with one exception. The splint with 71.13% mass performed the best in heat dissipation.

In general, it was observed that the deflection results had not a perfect correlation with the heat dissipation of the splints. At one end, the original splint with 100% mass, performed best mechanically, while the 71.13% mass splint performed best in heat dissipation. Therefore, a trade-off analysis is required to opt for the most appropriate splint.

The trade-off results are shown in **Figure 13** that the topology-optimized splint with 71.13% mass-produced reasonable mechanical properties
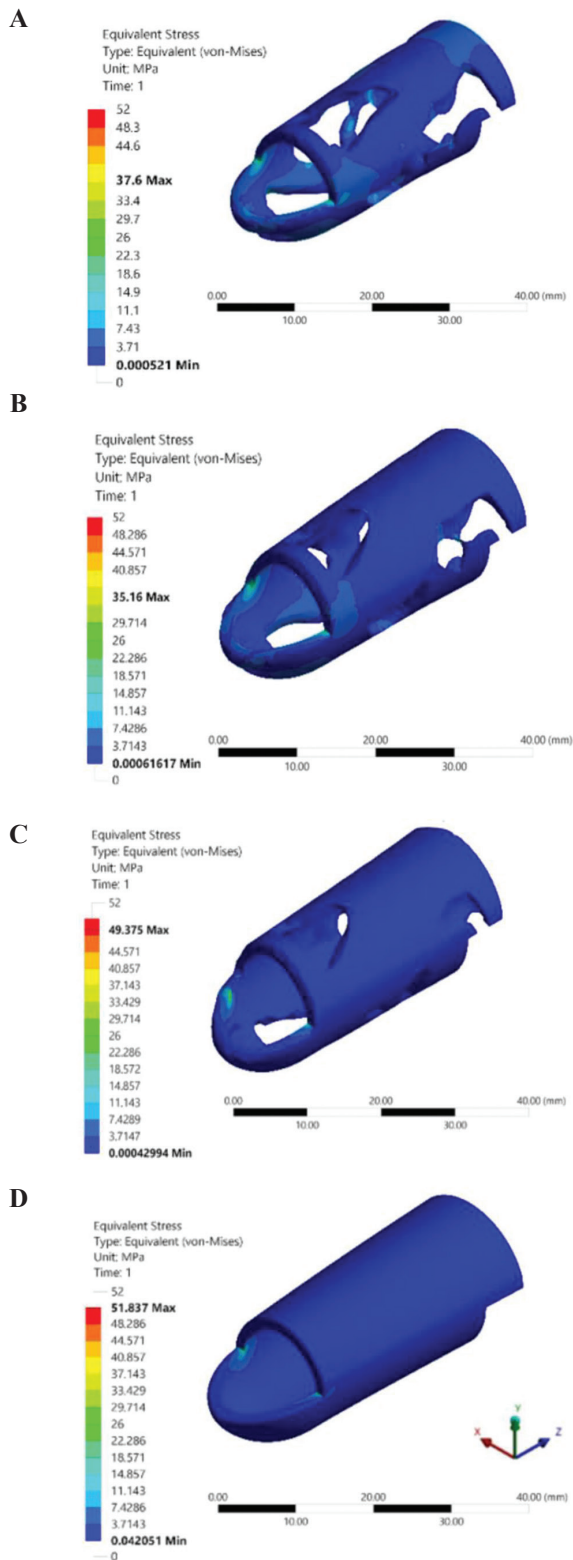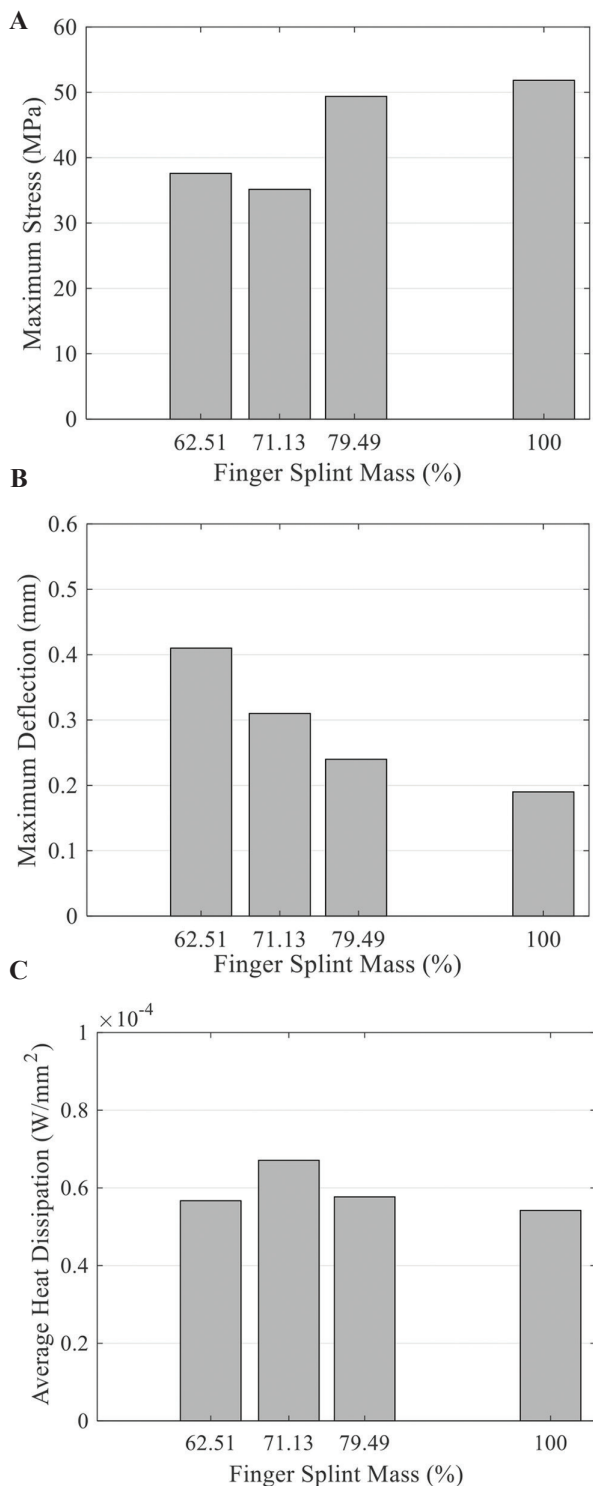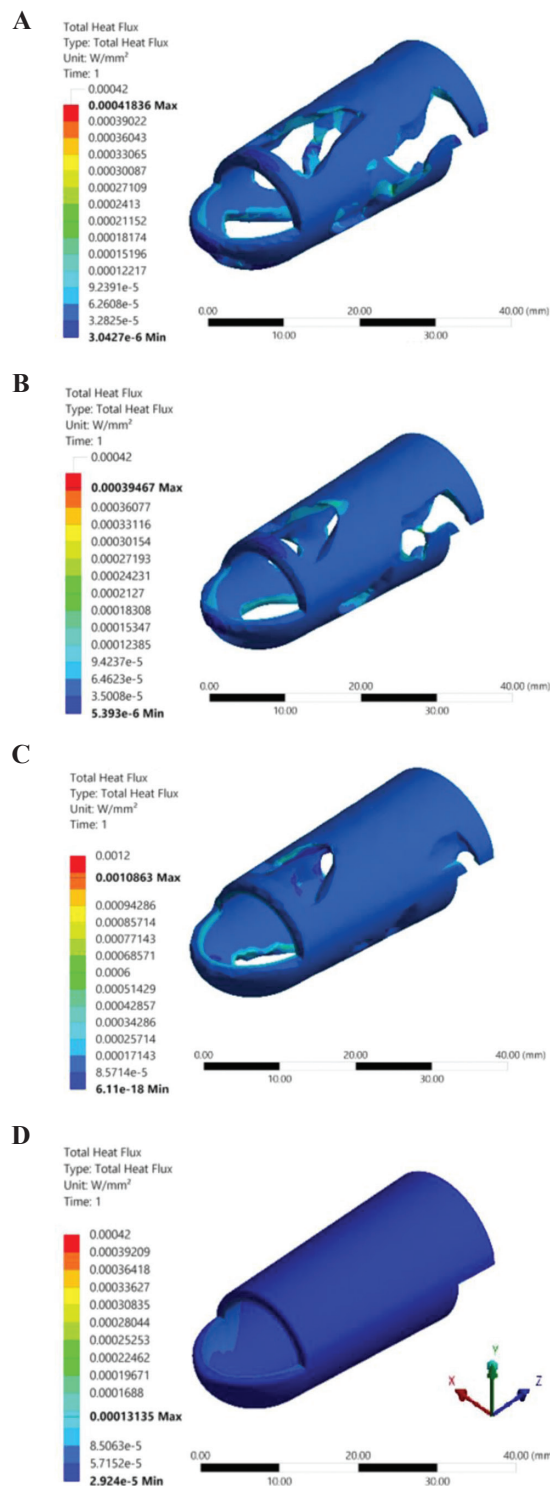
Figure 9. Stress simulation results of topology-optimized (A) 62.51% mass, (B) 71.13% mass, (C) 79.49% mass, and (D) original three-dimensional-printed 100% mass, splints.
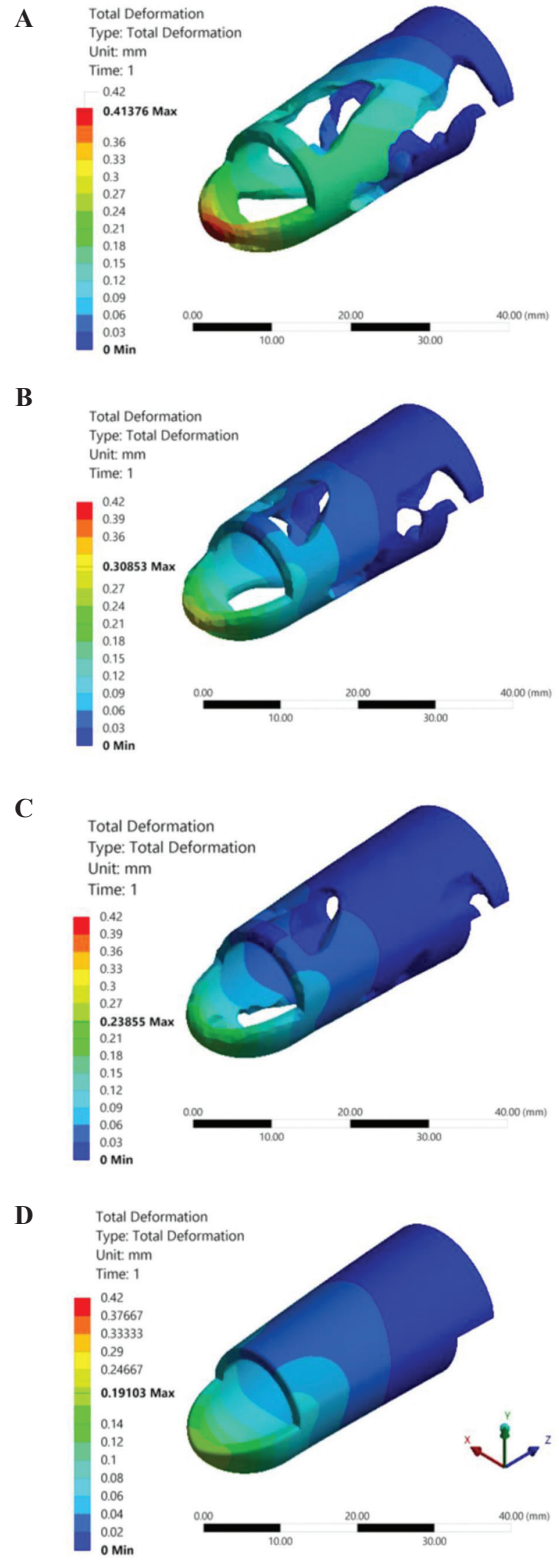
Figure 10. Deflection simulation results of topology-optimized (A) 62.51% mass, (B) 71.13% mass, (C) 79.49% mass, and (D) original three-dimensional-printed 100% mass, splints.
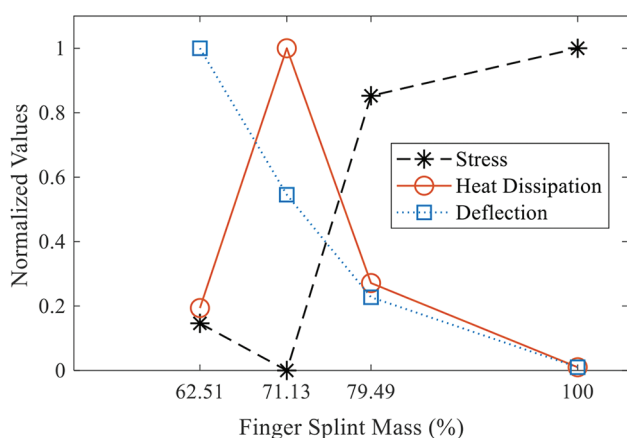
Figure 11. Comparison of the three-dimensional-printed splints simulation results (A) Maximum Equivalent (von-Mises) stress; (B) maximum deflection; (C) average heat dissipation.

Figure 12. Heat distribution simulation results of topology-optimized (A) 62.50% mass, (B) 71.13% mass, (C) 79.49% mass, and (D) original three-dimensional-printed 100% mass, splints.

considering both maximum stress and deflection values while reducing the heat trapped around the finger by a significant amount. This splint is simpler to print than lower percentage mass splints that can require more printing support structures. It was found that inevitably reducing the amount of material in a load-bearing finger splint would increase the deflection of it. However, when the distribution of that material is chosen to optimize the stiffness in that situation, the deflection value was low enough to justify its use.

For verifying the simulation results, some experiments were carried out to find the maximum deflection that occurred at the tip of the 3D-printed splints. A set up, as shown in **Figure 14A**, was used


Figure 13. A trade-off among deflection, stress, and heat dissipation of three-dimensional-printed splints.

in an Instron 300LX (Instron, High Wycombe, UK) to measure the average maximum deflection of the three splints from each design. The comparison results, shown in **Figure 14B**, imply good agreement of the experimental findings with the simulations.

Surface finish and appearance are important considerations in comfort and appeal to the user. The parameters that optimize the quality of 3D printing need to be explored in this area to compete with the thermoplastic hand molded thermoplastic splints. There are some complications on achieving more strength of splints through print orientations on the expense of losing the surface finish quality, which could be the subject for future work.

Investigation in the future needs to be undertaken into the duration of time before PLA splints begin to experience mechanical property decline. It should be investigated at what point in the lead up to hydrolysis does mechanical performance decline. Fatigue testing should be investigated in the future. Cyclic loading of a finger splint with sub-maximal loads may place a more realistic loading pattern on the splint than one large one off-load. In the day-to-day wearing of a finger splint, the user would apply small repeat loads into the splint. This over the course of the 6 – 8-week recovery period may cause degradation or decline in mechanical properties of the splint.

Measurements of the finger were taken with calipers. Taking seven dimensions of the
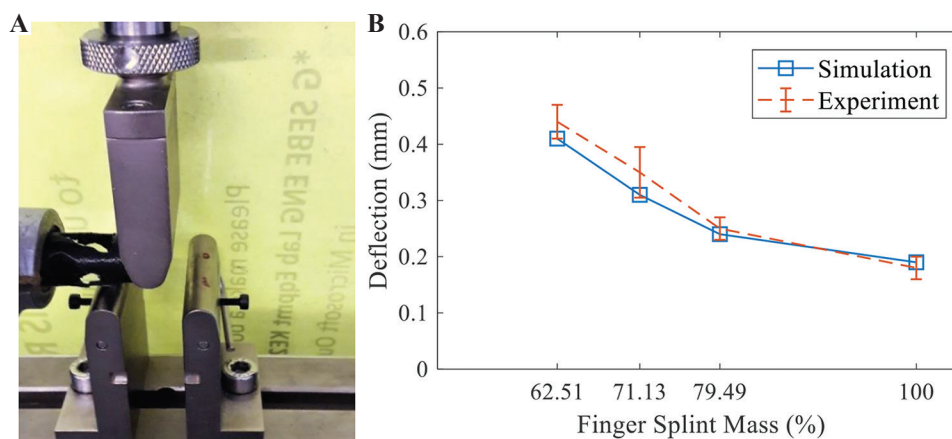
Figure 14. (A) A topology optimized three-dimensional-printed splint under deflection test; (B) comparison of experiments versus simulations of splints deflection.

finger to provide enough detail to get a highly specific customized splint to the user's finger. A progression for this project will be to use a 3D scanner to obtain the dimensions of the user's finger. This will provide an even higher level of accuracy and specificity to the patient.

4 Conclusion

In this work, a novel design of a patient-specific finger splint for a mallet finger treatment was proposed. The structure of the splint was fabricated in a size of a custom injured finger using AM. Utilizing FDM 3D printing provides a customizable fit specific to the patient. The FEA and TO were employed to create a splint with less material to reduce heat while conserving its satisfactory mechanical properties. This allows for much better breathability and less sweating for the patient, possibly lead to increase comfort for the duration of their recovery. Less material in the splint reduces the heat generated in the splint when in use, improving the comfort of the patient. Combining these two techniques optimizes mechanical properties and user comfort for the best chance of an optimal outcome for patients. This paper demonstrated how the use of engineering concepts and developing technologies could improve outcomes for patients in the treatment of mallet finger injury. The results of this project would pave the way for the medical industry to utilize superior advanced manufacturing and minimum materials that have been shape optimized to better serve their purpose while improving patient comfort.

References

1. Pegoli L, Pivato G, 2019, Mallet finger injuries. In: Sports Injuries of the Hand and Wrist. Springer, Berlin. pp. 1–13. DOI: 10.1007/978-3-030-02134-4_1.

2. Engdahl SM, Christie BP, Kelly B, *et al.*, 2015, Surveying the Interest of Individuals with Upper Limb Loss in Novel Prosthetic Control Techniques. *J Neuroeng Rehabil*, 12:53. DOI: 10.1186/s12984-015-0044-2.

3. O'Brien L, 2010, Adherence to Therapeutic Splint Wear in Adults with Acute Upper Limb Injuries: A Systematic Review. *Hand Ther*, 15:3–12. DOI: 10.1258/ht.2009.009025.

4. Young KJ, Pierce JE, Zuniga JM, Assessment of Body-powered 3D Printed Partial Finger Prostheses: A Case Study. *3D Print Med*, 5:7. DOI: 10.1186/s41205-019-0044-0.

5. Choi H, Seo A, Lee J, 2019, Mallet Finger Lattice Casts Using 3D Printing. *J Healthc Eng*, 2019:4765043.

6. Koo DS, Lee JR, 2017, The Development of a Wrist Brace using 3D Scanner and 3D Printer. *Fashion Text Res J*, 19:312–9. DOI: 10.5805/sfti.2017.19.3.312.

7. Żyluk A, Piotuch B, 2010, Treatment of Mallet Finger a Review. *Pol J Surg*, 82:243–50.

8. Bazavar M, Rouhani A, Tabrizi A, 2014, Simultaneous Dorsal Base Fracture and FDP Avulsion of Distal Phalanx of the Little Finger. *Arch Bone Joint Surg*, 2:63.

9. Tuttle HG, Olvey SP, Stern PJ, 2006, Tendon Avulsion Injuries of the Distal Phalanx. *Clin Orthop Relat Res*, 445:157–68.

10. Robinson LS, Sarkies M, Brown T, *et al.*, 2016, Direct, Indirect and Intangible Costs of Acute Hand and Wrist Injuries: A Systematic Review. *Injury*, 47:2614–26. DOI: 10.1016/j.injury.2016.09.041.

11. Brunet M, Haddad RJ, Sanchez J, *et al.*, 1984, How i Manage Sprained Finger in Athletes. *Phys Sportsmed*, 12:99–108. DOI: 10.1080/00913847.1984.11701926.

12. Imoto FS, Leão TA, Imoto RS, *et al.*, 2016, Osteosynthesis of Mallet Finger Using Plate and Screws: Evaluation of 25 Patients. *Rev Bras Ortop*, 51:268–73. DOI: 10.1016/j.rboe.2015.09.013.

13. O'Brien LJ, Bailey MJ, 2011, Single Blind, Prospective, Randomized Controlled Trial Comparing Dorsal Aluminum and Custom Thermoplastic Splints To Stack Splint For Acute Mallet Finger. *Arch Phys Med Rehabil*, 92:191–8. DOI: 10.1016/j.apmr.2010.10.035.

14. Berman B, 2013, 3D Printing: The New Industrial Revolution. *IEEE Eng Manag Rev*, 41:72–80. DOI: 10.1109/emr.2013.6693869.

15. Goh G, Yap YL, Tan HK, et al., 2019, Process-structure-properties in Polymer Additive Manufacturing Via Material Extrusion: A Review. *Crit Rev Solid State Mater Sci*, 45:1–21. DOI: 10.1080/10408436.2018.1549977.

16. Brenken B, Barocio E, Favaloro A, *et al.*, 2018, Fused Filament Fabrication of Fiber-reinforced Polymers: A Review. *Addit Manuf*, 21:1–16. DOI: 10.1016/j.addma.2018.01.002.

17. Blaya F, Pedro PS, Silva JL, *et al.*, 2018, Design of an Orthopedic Product by Using Additive Manufacturing Technology: The Arm Splint. *J Med Syst*, 42:54.

18. Yu C, Jiang J, 2020, A Perspective on Using Machine Learning in 3D Bioprinting. *Int J Bioprinting*, 6:95. DOI: 10.18063/ijb.v6i1.253.

19. Durgun I, Ertan R, 2014, Experimental Investigation of

FDM Process for Improvement of Mechanical Properties and Production Cost. *Rapid Prototyp J*, 20:228–35. DOI: 10.1108/rpj-10-2012-0091.

20. Bodaghi M, Noroozi R, Zolfagharian A, *et al*., 2019, 4D Printing Self-morphing Structures. *Materials*, 12:1353. DOI: 10.3390/ma12081353.

21. Rahim TN, Abdullah AM, Akil HM, 2019, Recent Developments in Fused Deposition Modeling-based 3D Printing of Polymers and their Composites. *Polym Rev*, 59(4):589-624. DOI: 10.1080/15583724.2019.1597883.

22. Jiang J, Xu X, Stringer J, 2019, Optimisation of Multi-part Production in Additive Manufacturing for Reducing Support Waste. *Virtual Phys Prototyp*, 14:219–28. DOI: 10.1080/17452759.2019.1585555.

23. Bodaghi M, Serjouei A, Zolfagharian A, *et al*., 2020, Reversible Energy Absorbing Meta-Sandwiches by 4D FDM Printing. *Int J Mech Sci*, 173:105451. DOI: 10.1016/j.ijmecsci.2020.105451.

24. Zolfagharian A, Kouzani A, Khoo SY, *et al*., 2018, 3D Printed Soft Parallel Actuator. *Smart Mater Struct*, 27:45019. DOI: 10.1088/1361-665x/aaab29.

25. Zolfagharian A, Kaynak A, Kouzani A, 2019, Closed-loop 4D-printed Soft Robots. *Mater Des*, 188:108411. DOI: 10.1016/j.matdes.2019.108411.

26. Jiang J, Xu X, Stringer J, 2018, Support Structures for Additive Manufacturing: A Review. *J Manuf Mater Process*, 2:64.

27. Gordelier TJ, Thies PR, Turner L, *et al*., 2019, Optimising the FDM Additive Manufacturing Process to Achieve Maximum Tensile Strength: A State-of-the-art Review. *Rapid Prototyp J*, 25:953-971. DOI: 10.1108/rpj-07-2018-0183.

28. Mohamed OA, Masood SH, Bhowmik JL, 2015, Optimization of Fused Deposition Modeling Process Parameters: A Review of Current Research and Future Prospects. *Adv Manuf*, 3:42–53. DOI: 10.1007/s40436-014-0097-7.

29. Wong JY, 2015, On-site 3D Printing of Functional Custom Mallet Splints for Mars Analogue Crewmembers. *Aerosp Med Hum Perform*, 86:911–4. DOI: 10.3357/amhp.4259.2015.

30. Cazon A, Kelly S, Paterson AM, *et al*., 2017, Analysis and Comparison of Wrist Splint Designs Using the Finite Element Method: Multi-material Three-dimensional Printing Compared to Typical Existing Practice with Thermoplastics. *Proc Inst Mech Eng H*, 231:881–97. DOI: 10.1177/0954411917718221.

31. Dhanwal DK, Dennison EM, Harvey NC, *et al*., 2011, Epidemiology of Hip Fracture: Worldwide Geographic Variation. *Indian J Orthop*, 45:15–22. DOI: 10.4103/0019-5413.73656.

32. Lee RJ, Mears SC, 2012, Greening of Orthopedic Surgery. *Orthopedics*, 35:e940–4. DOI: 10.3928/01477447-20120525-39.

33. Teo AJ, Mishra A, Park I, *et al*., 2016, Polymeric Biomaterials for Medical Implants and Devices. *ACS Biomater Sci Eng*, 2:454–72.

34. Jiang J, Xu X, Stringer J, 2019, Optimization of Process Planning for Reducing Material Waste in Extrusion Based Additive Manufacturing. *Robot Comput Integr Manuf*, 59:317–25. DOI: 10.1016/j.rcim.2019.05.007.

35. Liu X, Song R, Zhang W, *et al*., 2017, Development of Eco-friendly Soy Protein Isolate Films with High Mechanical Properties Through HNTs, PVA, and PTGE Synergism Effect. *Sci Rep*, 7:1–9. DOI: 10.1038/srep44289.

36. Yang R, Chen C, 1996, Stress-based Topology Optimization. *Struct Optim*, 12:98–105.

37. Zolfagharian, A., Denk, M., Bodaghi, M, *et al*., 2019, Topology-optimized 4D Printing of a Soft Actuator. *Acta Mech Solid Sin*, 1:1-13. DOI:10.1007/s10338-019-00137-z.

38. Labanda, S.R, 2015, Mathematical Programming Methods for Large-scale Topology Optimization Problems. PhD Thesis, DTU.

39. Bendsøe MP, 2009, Topology Optimization. Springer, Berlin.

40. Price MJ, Trbovich M, 2018, Thermoregulation following spinal cord injury. In: Handbook of Clinical Neurology. Elsevier, Amsterdam. pp. 799–820. DOI: 10.1016/b978-0-444-64074-1.00050-1.

41. Stevens M, 2016, Human Body Heat as a Source for Thermoelectric Energy Generation, Submitted as Coursework for PH240. Stanford University, United States.